



PAPER

Spectral and temporal characterization of sleep spindles—methodological implications

RECEIVED
31 August 2020REVISED
26 January 2021ACCEPTED FOR PUBLICATION
22 February 2021PUBLISHED
16 March 2021Javier Gomez-Pilar^{1,2,*} , Gonzalo C Gutiérrez-Tobal^{1,2} , Jesús Poza^{1,2,3} , Stuart Fogel^{4,5}, Julien Doyon^{6,7}, Georg Northoff^{5,8} and Roberto Hornero^{1,2,3} ¹ Biomedical Engineering Group, University of Valladolid, Paseo de Belén, 15, 47011 Valladolid, Spain² Centro de Investigación Biomédica en Red en Bioingeniería, Biomateriales y Nanomedicina, (CIBER-BBN), Valladolid, Spain³ IMUVA, Mathematics Research Institute, University of Valladolid, Valladolid, Spain⁴ School of Psychology, University of Ottawa, Ottawa, Canada⁵ Mind, Brain Imaging and Neuroethics, Institute of Mental Health Research, University of Ottawa, Ottawa, Canada⁶ Functional Neuroimaging Unit, Centre de Recherche de l'Institut Universitaire de Gériatrie de 8 Montréal, Montreal, Canada⁷ McConnell Brain Imaging Centre and Department of Neurology and Neurosurgery, McGill University, Montreal, Canada⁸ Mental Health Center, Zhejiang University School of Medicine, Hangzhou, Zhejiang, People's Republic of China

* Author to whom any correspondence should be addressed.

E-mail: javier.gomez@gib.tel.uva.es**Keywords:** sleep spindles, slow oscillations, state-dependence, EEG, spectral and temporal featuresSupplementary material for this article is available [online](#)**Abstract**

Objective. Nested into slow oscillations (SOs) and modulated by their up-states, spindles are electrophysiological hallmarks of N2 sleep stage that present a complex hierarchical architecture. However, most studies have only described spindles in basic statistical terms, which were limited to the spindle itself without analyzing the characteristics of the pre-spindle moments in which the SOs are originated. The aim of this study was twofold: (a) to apply spectral and temporal measures to the pre-spindle and spindle periods, as well as analyze the correlation between them, and (b) to evaluate the potential of these spectral and temporal measures in future automatic detection algorithms. *Approach.* An automatic spindle detection algorithm was applied to the overnight electroencephalographic recordings of 26 subjects. Ten complementary features (five spectral and five temporal parameters) were computed in the pre-spindle and spindle periods after their segmentation. These features were computed independently in each period and in a time-resolved way (sliding window). After the statistical comparison of both periods, a correlation analysis was used to assess their interrelationships. Finally, a receiver operating-characteristic (ROC) analysis along with a bootstrap procedure was conducted to further evaluate the degree of separability between the pre-spindle and spindle periods. *Main results.* The results show important time-varying changes in spectral and temporal parameters. The features calculated in pre-spindle and spindle periods are strongly and significantly correlated, demonstrating the association between the pre-spindle characteristics and the subsequent spindle. The ROC analysis exposes that the typical feature used in automatic spindle detectors, i.e. the power in the sigma band, is outperformed by other features, such as the spectral entropy in this frequency range. *Significance.* The novel features applied here demonstrate their utility as predictors of spindles that could be incorporated into novel algorithms of automatic spindle detectors, in which the analysis of the pre-spindle period becomes relevant for improving their performance. From the clinical point of view, these features may serve as novel precision therapeutic targets to enhance spindle production with the aim of improving memory, cognition, and sleep quality in healthy and clinical populations. The results evidence the need for characterizing spindles in terms beyond power and the spindle period itself to more dynamic measures and the pre-spindle period. Physiologically, these findings suggest that spindles are more than simple oscillations, but nonstable oscillatory bursts embedded in the complex pre-spindle dynamics.

1. Introduction

Human neural activity manifests characteristic and intricate patterns that depend on brain state. This complex structure of neural dynamics is not limited to wakefulness, as demonstrated by several studies focusing on sleep states [1–4]. One of the main properties of neural activity during sleep is the intrinsic macroarchitecture, which characterizes two well-differentiated stages: rapid eye movement (REM) and non-REM (NREM). According to the American Academy of Sleep Medicine (AASM), NREM, in turn, consists of three different stages [5]: N1, N2, and N3. Even within the same sleep stage, a complex microarchitecture exists, which comprises both slow and fast nonstationary phasic burst-like events [6], as well as tonic periods; impacting both the ongoing spectral and temporal patterns of the neural activity. Due to the transitory nature of these phasic events, the use of techniques with a high temporal resolution becomes necessary. For this reason, the electroencephalogram (EEG) is the gold-standard approach to assess neural microarchitecture during sleep.

Distant areas of the brain (e.g. the thalamus and cortex) communicate actively while sleeping. During NREM sleep, this highly structured and coordinated communication occurs in a burst mode, whereby greater functional connectivity as compared to wake is observed in particular networks such as the dorsal attention network [7], while other networks such as the visual, auditory, somatomotor, and default mode networks remain unchanged [7]. Accordingly, different brain waves such as spindles and slow oscillations (SOs) are generated by rhythmic thalamocortical neuronal firing. These complex interactions contain information that may reflect their function, encoded in their temporal structure. Among them, sleep spindles are sparking growing interest due to the increasing evidence on their role in a number of cognitive processes during sleep [8–11]. Spindles, EEG hallmarks of N2, are recognizable bursts of 11–16 Hz (sigma frequency activity) in the EEG [10]. Spindles are not isolated events. In fact, spindles are generally nested with other oscillations in a distinctive hierarchical manner, in which SOs coordinate the organization of a triplet of waves: SO themselves, spindles, and ripples [12]. SOs are oscillations around 0.75 Hz that facilitate the production of spindles [12]. Spindles are modulated by the up-state of the SO which, in turn, facilitates the production of high frequency bursts around 100 Hz in the hippocampus, called ripples [12, 13]. Through the dynamic interaction of these three events, information is exchanged between distributed neocortical and subcortical sites allowing for a variety of cognitive functions, some of them not fully understood yet [12, 14].

Despite the complex nested hierarchy of electrophysiological waves and bursts in which spindles appear to be embedded, most studies only have

described spindles in basic statistical terms (i.e. duration of spindles, number of spindles per minute, or evolution of their appearance throughout the night) [12] or, in some cases, by a distinction of spindles (i.e. fast and slow) based on their oscillatory frequency [15, 16]. Much less often, other measurements have been used for the characterization of spindles, such as spectral power in the sigma band or coherence [17], and interactions with other oscillatory frequencies [18]. This provides a rather limited insight into the dynamics of spindles. Investigations on the awake state point out the importance of using complementary spectral and temporal features like irregularity (indexed by spectral entropy (SE) [19] or sample entropy [20]), spectral distribution (indexed by median frequency (MF) [21] or power law exponent (PLE) [22]), complexity (indexed by Lempel–Ziv [23]), variability (indexed by central tendency measure (CTM) [24] and trial-to-trial variability (TTV) [25]) and periodicity (indexed by autocorrelation window (ACW) [26]), for describing neural activity changes during rest and/or task states. Due to the nature of the spindle as a frequency burst of EEG activity, it is expected that not only the relative power (RP) changes during the spindle, but also other characteristics such as those previously mentioned. Most notably, dynamic changes in these features can, in part, be observed in awake state already prior to the onset of the actual stimulus or task [22, 25], that is, in the pre-stimulus period. Taking these lessons from awake states, one may raise the question whether the spindle dynamics are characterized by somewhat analogous changes in both pre- and post-spindle intervals. Specifically, one would hypothesize changes in the dynamics of the pre-spindle period to precede the actual onset of the spindle. That is even more likely given that the long cycle duration of the SOs, as known to be instrumental in spindle generation [12], may cut across the distinction of pre- and post-spindle periods. Therefore, the characterization of both pre-spindle and post-spindle periods in order to trace their changes over time could serve the purpose to track the dynamics of spindle generation which, as we will raise in the following, may improve spindle detection.

For dimensionality and scalability reasons, most of the spindle-related studies rely on their automatic detection. Any potential bias from these algorithms would transfer to statistical analyses, which could explain the infrequent lack of correlation between spindle features and specific cognitive traits (correlated in other studies) [15]. However, the performance of automatic detectors has been shown to be worse than the performance of manual labeling by both expert and non-expert groups [27]. A possible cause of the underperforming of automatic spindle detectors compared to manual scoring could consist in the lack of considering spindle dynamics by including their changes from pre- to post-spindle period.

Including pre- and post-spindle dynamics in automatic algorithms may therefore hold the promise to improve the reliability of spindle detection.

Many detection approaches are based almost exclusively on detecting an increase of power in the sigma frequency band. The particular algorithm behind each method varies significantly, ranging from analyses based on the wavelet transform [28, 29] and other transformations, such as Gabor [30], complex demodulation [31] or Fourier transforms [32], to the use of filters and statistical methods [33]. However, the description of the temporal dynamics of spindles should not be restricted to the amplitude of the spindle power itself and should also involve the pre-spindle period as that may, dynamically, modulate time-varying properties during the spindle period, thus, considering the hierarchical complex in which they are embedded. In particular, spindles are modulated by the SO and are nested in those oscillations. SOs are normally generated previously to the emergence of a spindle, phase-locked to them. Additionally, other features considering the changes in the dominant frequency, the width of the sigma band or the irregularity of the oscillations could enhance the performance of automatic spindle detectors.

Due to the particular relationship between spindles and SOs (generated previously to the spindle onset), we hypothesized that there would be a correlation between the features of the pre-spindle and spindle periods. We also propose different spectral and/or temporal features besides power in the sigma band that can serve as potential therapeutic targets to enhance spindles with the aim of improving cognition. Furthermore, by improving the characterization of spindles, higher performance automatic spindle detectors could be developed, reducing the bias in subsequent analyses. In order to test these hypotheses, the objective of this study is twofold: (a) to apply spectral and temporal measures to the pre-spindle and spindle periods, as well as analyze the correlation between them, and (b) to evaluate the potential of these spectral and temporal measures in future automatic detection algorithms. For this purpose, EEG signals from overnight polysomnography (PSG) were acquired. Then, after the automatic spindle detection, five spectral and five temporal features were computed for pre-spindle and spindle periods both individually and in a time-resolved way. Finally, in order to assess the feasibility of using these measures in future automatic spindle detectors, the degree of separability between the pre-spindle and spindle periods was assessed using the evaluated measures as a naïve classifier.

2. Materials and methods

2.1. EEG recordings and sleep stage labeling

A total of 26 young adults (26.00 ± 6.69 years, 18 women) free from sleep and neurological disorders

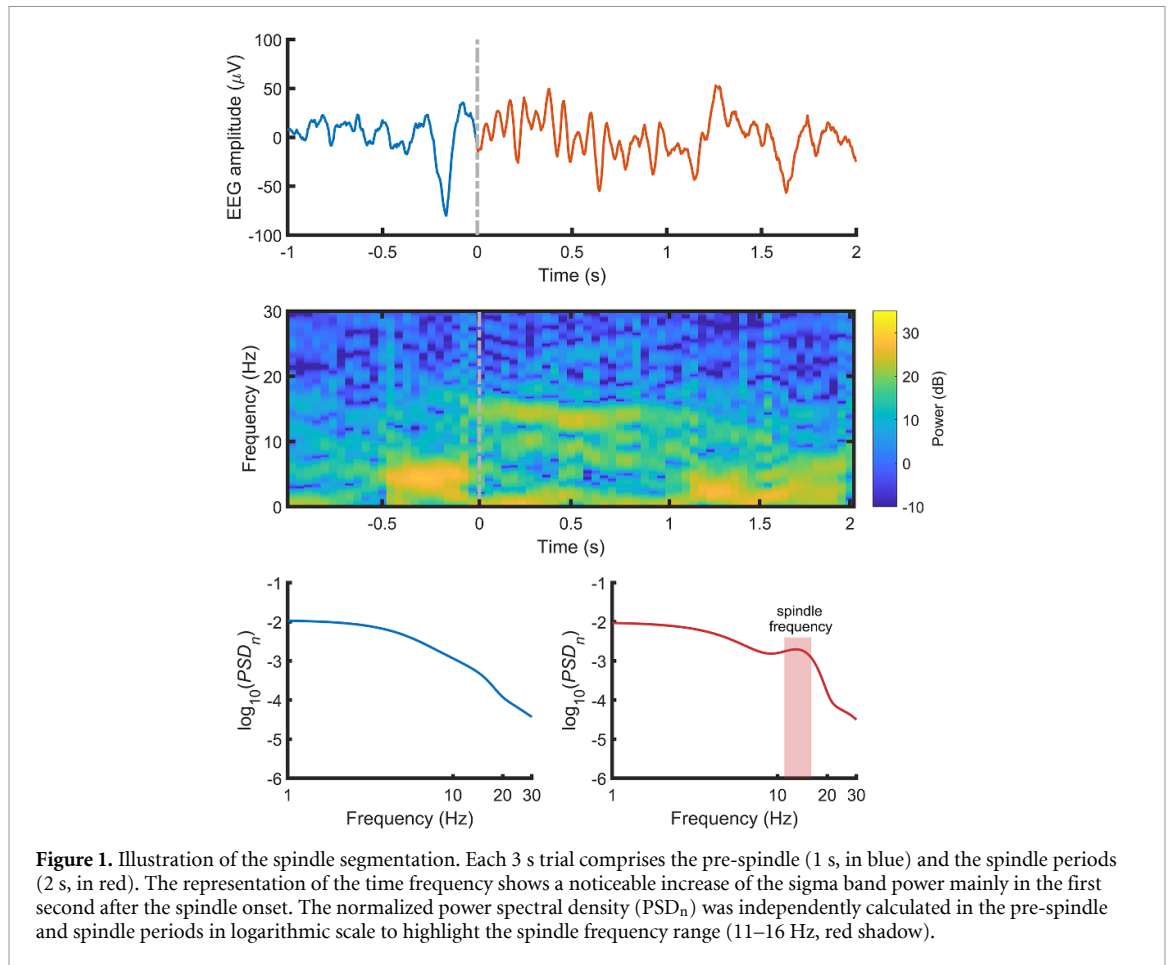
were recruited in this study. After obtaining informed written consent from the participants, physiological signals were recorded during an overnight PSG using Embla Titanium PSG systems (Natus, San Carlos, CA). EEG was acquired at a sampling rate of 256 Hz, while keeping the impedances under 5 k Ω . Thirteen gold-plated electrodes were placed according the international 10–20 system (scalp locations: F3, Fz, F4, C3, Cz, C4, P3, Pz, P4, Oz, M1 and M2) and referenced to FPz and AFz for the ground. Ethical approval was obtained from the Research Ethics Board at the *Institut Universitaire de Gériatrie de Montréal*.

Once acquired, EEG signals were re-referenced offline to the average activity of the mastoid derivations (M1 and M2) for sleep stage scoring and subsequent analysis. RemLogic analysis software (Natus) was used to label the sleep stages (wake, N1, N2, N3, REM) in epochs of 30 s and to mark noisy segments (excluded from further analysis) in, as recommended by the AASM [5].

2.2. Automatic spindle detection and segmentation

An automatic spindle detection method implemented in EEGLAB [34] was carried out on the cortical midline electrodes (Fz, Cz and Pz) using a well-established [35, 36] and validated method [31]. In brief, the algorithm is based on a complex demodulation method, where a carrier frequency in the center of the spindle range (13.5 Hz) is shifted towards the origin by multiplying the signal, $x[n]$, by e^{-iwn} , being i the imaginary unit and w the angular frequency. The resulting signal, $y[n]$, is then low-pass filtered (infinite impulse response, 4th order Butterworth filter) in both forward and reverse directions (zero-phase digital filtering), removing the frequency component outside the band of interest [31]. Finally, spindle events were automatically detected when the amplitude of $y[n]$ on the normalized signal is higher than the 99th percentile [31]. For this study, the spindles with a duration larger than 0.5 and shorter than 2 s were selected, since they represent more than the 99% of the total number of spindles. The Matlab code for automatic spindle detection is freely available at: https://github.com/stuartfogel/detect_spindles. Results are reported for slow spindles detected at Fz (11–13.5 Hz), fast spindles at Pz (13.5–16 Hz) and full-bandwidth spindles at Cz (11–16 Hz).

Once the spindles were detected, a band-pass finite impulse response filter (Hamming window) between 1 and 30 Hz was applied for increasing the signal-to-noise ratio in a frequency range that sufficiently encompasses SOs and spindles. To verify that all 30 s epochs contaminated by artifacts were removed, an adaptive epoch rejection protocol previously validated was applied [37, 38]. This algorithm uses a statistical-based thresholding method to remove the noisy epochs following a two-step process. First, the mean and standard deviation (SD) of each channel was computed. Then, those



epochs that exceeded $\text{mean} \pm 4 \times \text{SD}$ in at least two channels were discarded.

Finally, spindles were segmented from 1 s before to 2 s after the spindle onset (time range: $[-1 \ 2]$ s). Figure 1 illustrates this segmentation, while showing the power spectral density (PSD) (Welch method) in the pre-spindle and spindle periods. The validation of preprocessing and spindle detection procedures was tested in a previous work [39].

2.3. EEG processing

With the aim of thoroughly characterizing spindles, both spectral and temporal measures were applied in two different ways: (a) calculation in a time-resolved way using a sliding window (window length of 0.5 s, overlap 90%), and (b) independent calculation during the pre-spindle ($[-1 \ 0]$ s) and spindle ($[0 \ 2]$ s) periods.

The selected ten measures (five spectral and five temporal parameters) uncover diverse properties that provide an extensive characterization of neural activity; from the more typical ones employed in previous spindle studies (such as RP in the sigma band) to measures not applied before in this context (e.g. Lempel–Ziv complexity (LZC), entropy and PLE). Below, we provide definitions and procedures to compute each of them. Figure 2 depicts the overall workflow followed for the analyses in this study.

2.3.1. Spectral features

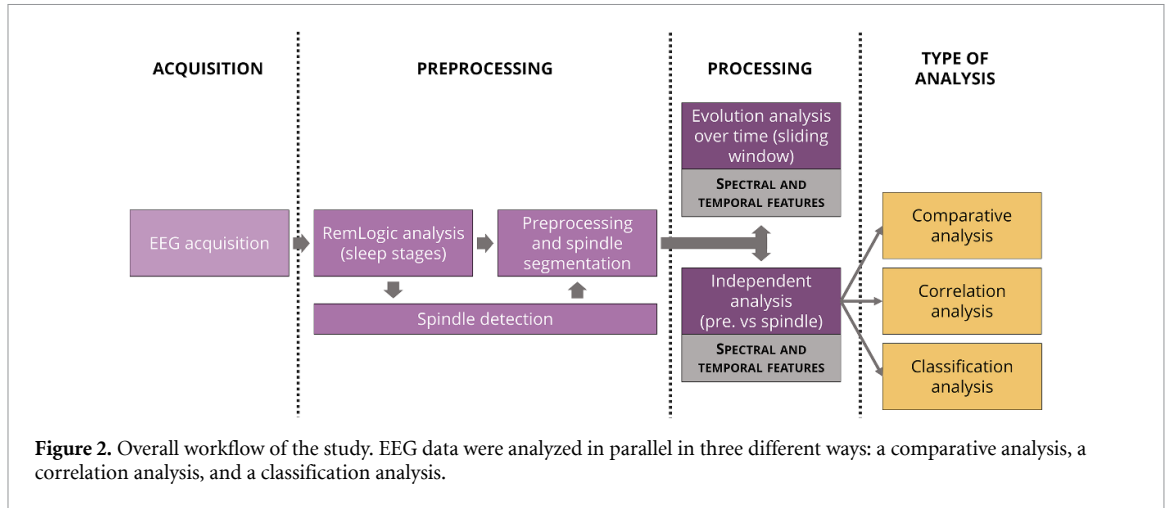
Brain dynamics are reflected in the spectral components of the EEG. They can be evaluated using the PSD of such signals. For that purpose, the Welch method was applied to each of the spindle trials [40]. In particular, we used a Hamming window with 50% overlap and 2^{12} as the number of points for the Fourier transform of each window. Then, the PSD was divided by the sum of its amplitude values, resulting in a normalized PSD (PSD_n) that can be interpreted as a probability density function. Finally, five different spectral parameters were computed.

The first feature is the RP in the sigma band. This measure was chosen for being the most extended feature both in characterizing spindles [41, 42] and in their automatic detection [31–33]. It can be defined as:

$$RP = \sum_{f=f_1}^{f_2} PSD_n(f), \quad (1)$$

where f_1 and f_2 are the frequency limits, which were set to 11 and 16 Hz, respectively (i.e. sigma band).

In order to assess not only the power, but also the shape of the PSD function, SE was used. SE is a measure of the irregularity of the signal, with values closer to 1 as the signal becomes more irregular, i.e. with a more balanced distribution of spectral components [19]. SE is formally defined as:



$$SE = \frac{-1}{\ln(N)} \sum_{f=f_1}^{f_2} PSD_n(f) \cdot \ln(PSD_n(f)), \quad (2)$$

being N the number of points of the PSD_n (i.e. 2^{12}).

Since the shape of the PSD function could have relevant information to characterize spindles, f_1 and f_2 were set to 1 and 30 Hz, respectively, defining the SE for the whole spectrum. Nonetheless, we also considered important a special focus on the sigma band, since the distribution of the spectral components in that frequency range is relevant and most apparent (see figure 1). For that reason, the SE was also computed in such frequency band by setting f_1 and f_2 to 11 and 16 Hz, respectively. It is important to note that the frequency limits of the analyzed signal influence in the final outcome of SE, since it depends on the number of the peaks in the analyzed spectrum, the degree of dominance of a such peaks, and their peakedness (relative to the bandwidth of the analyzed spectrum) [43].

The oscillation speed of the spindle trials was assessed by a summary measure termed MF. It is defined as the frequency in which the PSD area is divided in two equal halves [44]. The mathematical definition of MF is:

$$\frac{1}{2} \sum_{f=f_1}^{f_2} PSD_n(f) = \sum_{f=f_1}^{MF} PSD_n(f), \quad (3)$$

with f_1 and f_2 set to 1 and 30 Hz, respectively.

The last spectral feature computed in this study was the PLE. The PSD of most the EEG recordings can be fairly adjusted to the decreasing exponential function, with a similar trend than the pink noise [25]. Thus, the PLE would correspond to the exponent of that function:

$$PSD_n(f) \propto e^{-PLE \cdot f}. \quad (4)$$

Despite being a spectral measure, it also provides an estimation of the fractal organization of the signal,

where the faster (and also weaker) spectral components are nested within the slower (and higher) ones [25]. In simple terms, PLE measures the balance of the high and low frequencies. It is defined as the absolute value of the slope of the PSD regression line when it is represented using a log–log scale (see figure 1 at the bottom). Higher values of PLE mean strong dominance of the lower frequencies over the higher frequencies [25].

2.3.2. Temporal features

Spectral features can be complemented by time-varying and nonlinear dynamics computed over the signal in the time domain. Despite some of these features have proven to be useful in other contexts [45, 46], to the best of our knowledge none of them have been previously used for characterizing sleep spindles, with the exception of the TTV which has only been recently applied [39].

The temporal measures were calculated after a z-score normalization of each trial, thus minimizing the variability on electrodes impedance. As for the spectral measures (except for the RP and SE in the sigma band), the temporal features were computed in the broadband, thus providing a joint and complementary vision of how neuronal dynamics change due to the generation of spindles in the whole spectrum. The first one was the LZC, a nonparametric measure of complexity related to the rate of occurrence of distinct subsequences (i.e. patterns) in a given time series [47, 48]. Before calculating LZC, the signal, $x[i]$, is binarized into a new sequence (P) using a threshold (T) applied to the signal broadband, as follows:

$$P = s(1), s(2), \dots, s(n) \quad (5)$$

where

$$s(i) = \begin{cases} 0, & \text{if } x(i) < T \\ 1, & \text{otherwise} \end{cases}. \quad (6)$$

We used a median as the threshold, since it has been commonly applied in previous biomedical studies because its robustness to outliers [49]. The sequence P is then scanned, and a complexity index, $c(m)$, increases every time a new subsequence is found. Finally, LZC is normalized to reflect the arising rate of new patterns in the sequence, as follows [48]:

$$\text{LZC} = \frac{c(m)}{m/\log_2(m)}, \quad (7)$$

where m is the length of the time series. Further details of this algorithm are described in the supplementary material (available online at stacks.iop.org/JNE/18/036014/mmedia).

As the signal irregularity was previously estimated from the spectral point of view, its quantification in the temporal domain was also considered. Thus, sample entropy (SampEn) was computed for all the time series. SampEn is a nonlinear measure that quantifies the signal irregularity by estimating the predictability of the time series through the evaluation of the presence of repetitive patterns. The algorithm has two parameters that must be tuned according to the nature of the data: the embedding dimension (m) and the tolerance factor (r). As in previous studies and due to the good statistical reproducibility, we used: $m = 1$ and $r = 0.25$ times SD [46, 50]. Further details of this algorithm are detailed in the supplementary material and in [51].

It is common to find spindles embedded in SO, which usually show higher amplitude on average than the rest of the EEG activity. Therefore, the quantification of the variability of the signal amplitude over time can provide useful information for the characterization of spindles and their proximities. This can be analyzed using the CTM. It is computed selecting a circular region of radius r in a first-order difference plot. Then, the observations that fall inside the region delimited by the circle are summed and divided by the total number of observations [52]. In this study, a radius $r = 0.1$ was heuristically selected.

It has been reported that the frequency of the spindle is not constant throughout the spindle itself [53], but that the center frequency can vary within the sigma band, usually showing a decelerating pattern (negative chirping) [54]. This is reflected in the recurrence or periodicity of the signal that can be quantified by the ACW [55]. The ACW accounts for the full-width-at-half-maximum of the temporal autocorrelation function, providing an index of the periodicity of power fluctuations.

The last of the temporal measures used in this study was the TTV. This measure was previously used in the context of spindles, revealing the dependence of the spindle variability with the frequency [39]. Here, TTV was computed in the broadband (i.e. 1–30 Hz) to summarize the spindle variability across trials. It is

calculated as the SD across trials normalized by the SD at the spindle onset, as follows:

$$\text{TTV}[n] = \frac{\text{std}(x[n]) - \text{std}(x[0])}{\text{std}(x[0])} \quad (8)$$

where $\text{std}(\cdot)$ represents the SD and $x[0]$ is the EEG signal at the spindle onset. Finally, the root mean square of the TTV index was computed to provide a single value per trial accounting for the variability degree, named here as TTV energy:

$$\text{TTV}_{\text{energy}} = \sqrt{\frac{1}{N} \sum_i \text{TTV}[i]^2}. \quad (9)$$

2.4. Classification procedure

A receiver operating-characteristic (ROC) analysis was conducted to assess the degree of separability between the pre-spindle and spindle periods [56]. It was used along with a bootstrap procedure to accurately estimate the optimum threshold from which each extracted feature maximizes its discriminative ability between pre-spindle and spindle; thus, meaning an initial point to evaluate new detection algorithms hereafter. Accordingly, 1000 bootstrap replicates of the same size as the number of all pre-spindle and spindle epochs were formed for each extracted feature. This number allows for a proper estimation of the 95% confidence interval [57]. A uniform probability was used to select the values from the original dataset and this resampling was conducted with replacement, as indicated by the bootstrap 0.632 method [58]. Therefore, for each replicate, several values were selected more than once, whereas an equal number were not selected. These not selected values were used for the validation of results at each iteration [58].

The threshold maximizing separability in each replicate was obtained as the feature value that reached the closest distance to (1, 0) of the ROC curve [56]. The median of the 1000 thresholds obtained for each feature were chosen as the optimum. Additionally, the discriminative ability of the features was evaluated using sensitivity, specificity, accuracy, and area under the ROC curve (AROC). It is well-known, however, that the statistics obtained using only the instances not included in bootstrap replicates are downward estimations of the actual values [58]. Therefore, for each statistic t at each iteration, its value was computed considering both the instances included and not included in the replicates as follows [58]:

$$t = 0.632 \cdot t_{\text{ni}} + 0.368 \cdot t_i, \quad (10)$$

where t_i and t_{ni} are the values of the statistic considered in the instances included and not included in the corresponding replicate, respectively.

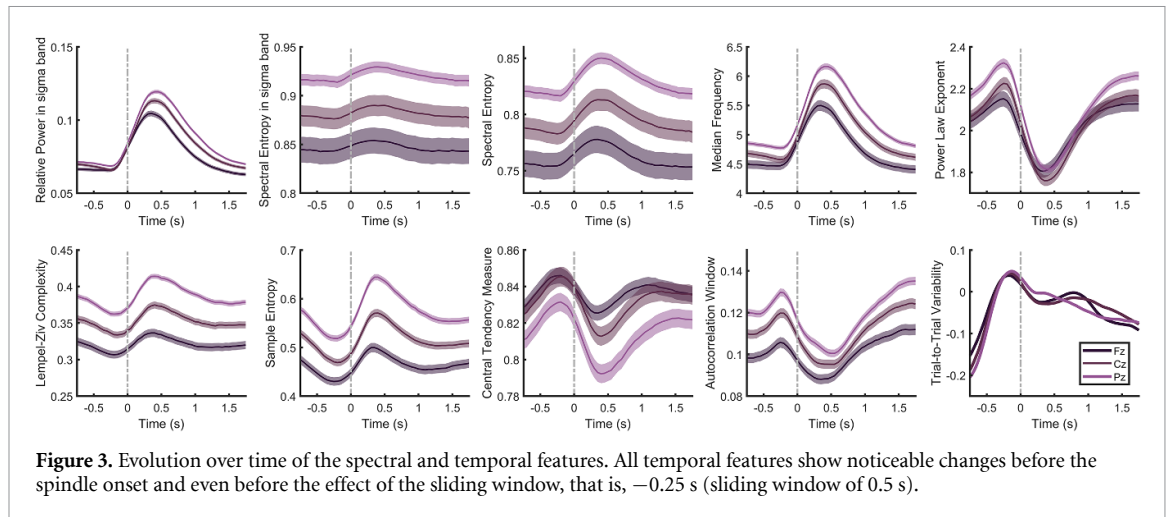


Figure 3. Evolution over time of the spectral and temporal features. All temporal features show noticeable changes before the spindle onset and even before the effect of the sliding window, that is, -0.25 s (sliding window of 0.5 s).

2.5. Statistical analysis

In a first step, Kolmogorov–Smirnov and Levene tests were used to check for normality and homoscedasticity of the obtained parameters. In the case where parametric assumptions were not met, Wilcoxon signed-rank test was used for pairwise comparisons. The computed p -values were corrected using the Benjamini–Hochberg procedure for controlling false discovery rate (FDR) [59].

We also analyzed the relationship between pre-spindle and spindle activity. Since we did not have an established hypothesis whether the relationship between the two neural activities would be linear or not, we applied the Spearman’s rho test to estimate the correlation.

All the signal processing, classification and statistical analysis were applied using in-house MATLAB (The MathWorks 2017b) scripts and the EEGLAB toolbox [34].

3. Results

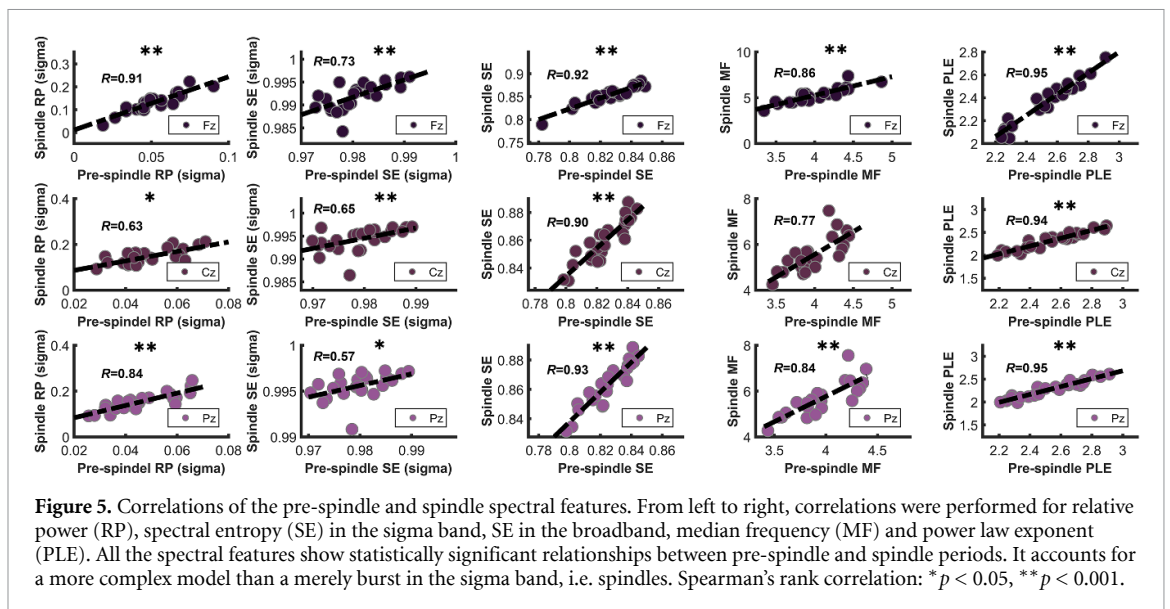
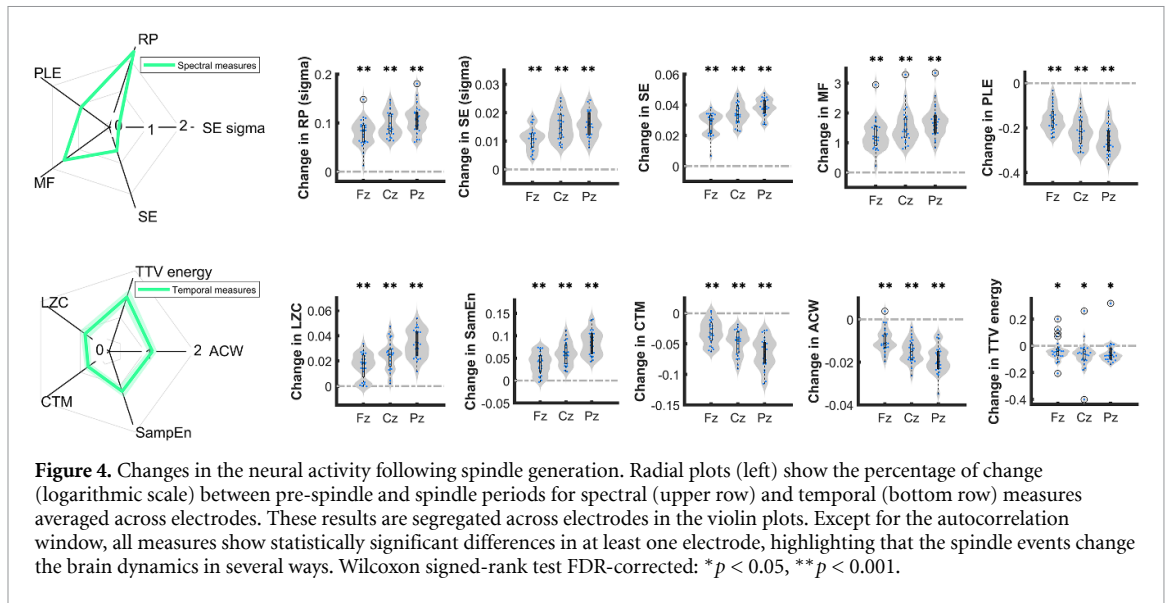
3.1. Spindle characterization

The temporal evolution of the frequency and time domain features was estimated for the three channels over the midline (Fz, Cz, and Pz). Remarkably, the spectral features show practically no changes during the pre-spindle period (figure 3), except for the PLE measure, which reveal a clear increase in its value followed by a decrease just before the start of the spindle; the latter being probably due to the beginning of the SO that is not detected by the other spectral measures. On the other hand, all the temporal characteristics show, to a greater or lesser extent, a pronounced change just before the spindle appears. It is particularly interesting that these variations are almost as noticeable as those produced during the spindle period. As expected, spectral and temporal features vary during the spindle period following the neural dynamics produced by the spindle burst. As the figure 3 shows, the most noticeable changes occur

in the first second after the spindle onset. In order to assess whether this is due to most of the spindles lasting 1 s or less [39], or due to other effect, the same analysis was repeated only with the spindles longer than 1 s. Since the changes in the features are not only restricted to the first second after the spindle onset (see figure S1 in the supplementary material), this suggests that the duration of the changes in the features is directly related to the spindle duration [39]. For that reason, and to remove the bias introduced by non-spindle-related activity, the spindle period was limited to the time interval $[0 \ 1]$ s for the subsequent analyses.

One can question whether the change between the pre-spindle and spindle periods is statistically significant for each of the characteristics or, on the contrary, these changes can be considered negligible. Figure 4 addresses this issue by subtracting the values of the features computed in the spindle period by those computed during the pre-spindle interval. As figure 4 shows, all the features achieve different degrees of statistical significance in all the channels. In terms of percentage changes (see figure 4 on the left), RP in sigma band is the feature with the highest changes, followed by both spectral and temporal features such as MF and TTV energy.

In view of the statistical differences in most of the features between pre-spindle and spindle periods, we focused on the study of the possible association between them. Thus, without *a priori* hypothesis of the nature of the possible association, Spearman’s rho test was applied for the correlation of the spectral (figure 5) and, temporal (figure 6) features. In general terms, despite overtly different pre-spindle and spindle periods (figure 3), statistically significant ($p < 0.001$) and strong ($R^2 > 0.7$) correlations were found for eight features (four spectral and four temporal features). Only the TTV did not obtain a significant correlation at Cz. These results highlight a strong association between the pre-spindle and the spindle periods. This high degree of correlation does



not necessarily indicate a high degree of separability between the two states, for which a classification analysis becomes necessary.

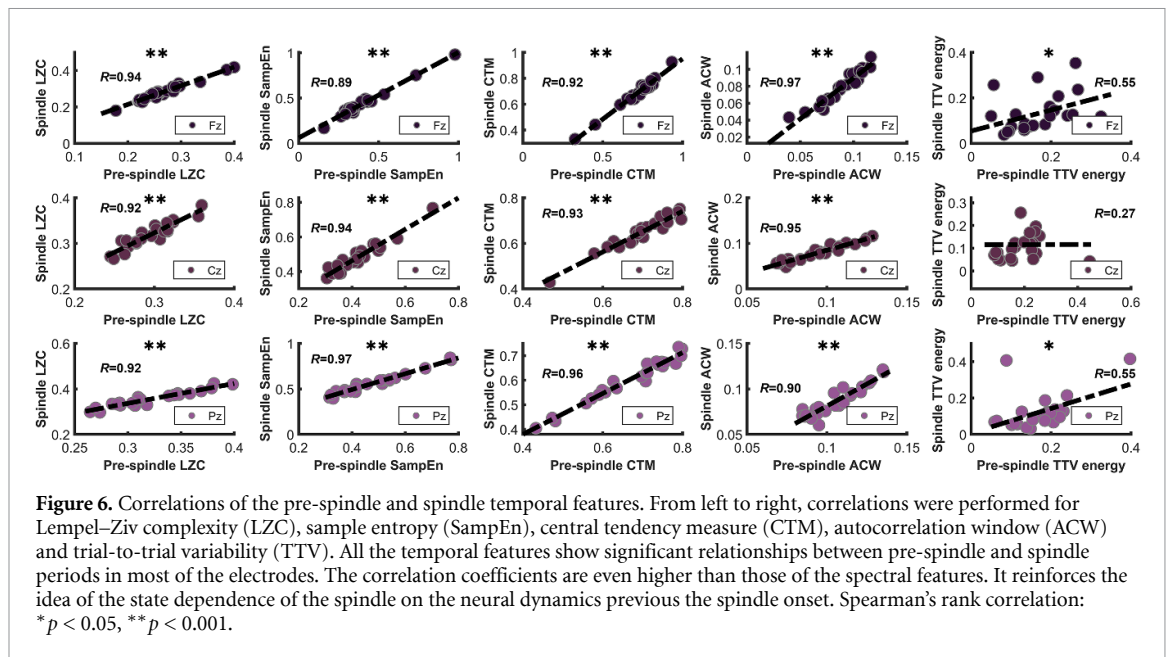
3.2. Separability between prespindle and spindle periods

Although the correlation analysis provides us with useful information on the degree of association between the analyzed brain states, it only offers indirect information on the degree of separability between them. To further analyze this aspect, a ROC curve for each feature was calculated by means of a bootstrap approach for full-bandwidth spindles at Cz. Statistical parameters independently computed for each feature are shown in table 1. Curiously, SE in the sigma band is the feature with the highest statistics in sensitivity (76.90%), accuracy (75.74%) and AROC (0.81). RP in sigma band was the feature with highest specificity (75.77%). The performance of the temporal features is similar to the spectral ones, with TTV reaching

a performance higher than 70% in all the statistics. These results are in line with those performed in Fz and Pz channels (see tables S1 and S2 in the supplementary material for these result), suggesting that the predictive capability of the pre-spindle period could be generalizable to other regions of the cortex where slow and fast spindles predominate, respectively.

4. Discussion

In the present study, we investigated the dynamics of the brain processes involved in spindle generation and its manifestation. The classical definition of a spindle provided by the AASM manual [5] considers them as bursts in the sigma band with a very specific physiological context (i.e. the sleep stage). However, this definition does not describe other important electrophysiological characteristics (related with the spatiotemporal dynamics) that could be important in their identification. Previous studies already provided



some details on these dynamics, such as the characteristic negative chirping of the spindles [54] or the synchronization and modulation between slow waves and spindles [60]. We here explored new properties taking advantage of the complementary vision of different characteristics (complexity, regularity, variability, etc) and comparing them to the classical feature for spindle characterization, i.e. RP.

Results showed important changes in various features evolving even before the spindle onset, and flattening 1 s after the beginning of the spindle (see figure 3) and probably linked with the mean duration of the spindles [39]. These changes in the brain dynamics showed significant differences both in spectral and in temporal features (figure 4). We then analyzed the correlation between the features computed on the pre-spindle and those computed on the spindle periods. We found high correlations both for the spectral and the temporal measures (see figures 5 and 6). Future studies should investigate on the causes for this high degree of association, despite overtly different pre-spindle and spindle periods (figure 3). Finally, we assessed the degree of separability between the pre-spindle and spindle periods. Results showed that features other than power in the sigma band, such as SE in sigma, could be jointly used as plausible features for automatically detecting sleep spindles, or potential therapeutic or experimental targets that could be leveraged to enhance spindle activity in healthy and clinical populations.

4.1. Methodological implications—usefulness in sleep spindles detectors

Until now, the definition of the spindle according to the AASM is based solely on the visually apparent increase of the EEG power in the sigma band, which results in an oscillation or burst at such a frequency

[5]. The sigma band partially overlaps with the alpha band (8–13 Hz), common at rest with eyes closed [61]. Therefore, alpha oscillations at, for example, 12 Hz are indistinguishable from slow spindles by an automatic algorithm based solely on power. This is a problem in all the automatic spindle detectors, but becomes particularly problematic in clinical population with alpha intrusion during sleep, or during micro-arousals due to e.g. sleep apnea, insomnia, or movement disorders [62]. An option to solve this issue is to use heuristic techniques to differentiate between the alpha band in resting awake and a spindle event. For instance, Yon *et al* implemented an algorithm that corrects for ‘alpha effects’ by removing slow spindles of frequency lower than 13 Hz when the power in parietal electrodes is higher than the power in the central ones [33]. However, these algorithms can lead to falsely rejecting slow spindles. We here propose an alternative procedure for automatic spindle detection, which would be based not only on the power in the sigma band but on the combination of different spectral and temporal features. The results show a greater ability of SE to distinguish between periods in which spindles are absent (pre-spindle period) and periods with spindles, as compared to the ability of the RP. Therefore, it is expected that a classifier combining both characteristics will achieve greater performance than the traditional detectors based on RP alone. On the basis of the previous ideas, this automatic detection could be addressed through the a set of complementary characteristics in methodologies based on machine learning or through algorithms that combine the information of different measures.

One would think that, due to the similarity between alpha oscillations and slow spindles, other features different from the power in sigma band may

Table 1. Assessment of the degree of separability between the pre-spindle and spindle periods for each feature. For each statistic, median and interquartile range were provided. The highest values for each statistic have been marked in bold.

	Spectral features					Temporal features				
	RP sigma	SE sigma	SE	MF	PLE	LZC	SampEn	CTM	ACW	TTV
Sensitivity (%)	65.77 (65.19, 67.48)	76.90 (75.69, 78.87)	58.68 (58.17, 59.18)	53.61 (51.03, 54.90)	53.49 (50.86, 58.79)	55.04 (54.74, 55.34)	56.61 (51.04, 57.25)	58.96 (56.02, 59.31)	56.97 (52.11, 57.27)	70.41 (39.34, 90.80)
Specificity (%)	75.77 (73.30, 76.54)	74.57 (72.87, 75.59)	70.49 (69.79, 70.96)	67.69 (65.87, 71.58)	59.42 (53.81, 62.40)	55.7 (55.4, 56.01)	55.64 (54.87, 61.53)	51.90 (51.59, 54.46)	69.26 (68.95, 77.02)	71.51 (41.93, 100.0)
Accuracy (%)	70.77 (70.39, 71.01)	75.74 (75.53, 75.93)	64.56 (64.31, 64.79)	60.78 (60.61, 61.56)	56.43 (56.15, 56.70)	55.36 (55.14, 55.59)	56.13 (55.89, 56.38)	55.44 (55.16, 55.68)	63.13 (62.90, 64.56)	70.03 (59.80, 78.90)
AROC	0.77 (0.76, 0.77)	0.81 (0.80, 0.81)	0.67 (0.61, 0.68)	0.64 (0.64, 0.65)	0.59 (0.59, 0.60)	0.56 (0.55, 0.56)	0.57 (0.57, 0.58)	0.56 (0.56, 0.57)	0.63 (0.63, 0.64)	0.77 (0.63, 0.89)

also be unable to discern between both types of waves. However, the negative chirping pattern in spindle events reported by other studies [54, 63] suggests that, while the power in the sigma band would not be able to find this slowing pattern, other characteristics can do so. Features, such as those related to the oscillation speed (MF) or the change of periodicity (ACW), help to support this hypothesis (see figure 3). By applying a time-resolved procedure, MF shows a decrease as the spindle fades, which is in line with the shift toward slower frequencies. This is also supported by the ACW. When the sleep spindle is generated, the central lobe of the autocorrelation function narrows, decreasing the ACW. Once the negative chirping occurs, the periodicity of the signal changes, resulting in an increase in ACW. In fact, many of these measurements help to recognize the type of spindle (fast or slow) detected. Thus, the evolution curves of figure 3 show a characteristic pattern in which the Cz channel is between the Fz and Pz channels. This is because spindles in the Cz channel were detected in the broadband, while slow and fast spindles were detected in Fz and Pz, respectively. Together, these results show that the spindles show different qualitative attributes (not only restricted to amplitude changes). These additional features could help in distinguishing the oscillatory patterns of alpha waves (or other brain activity, for that matter), as well as sleep spindles and their subtypes, thus, helping future spindle detectors to obtain higher performance. Further work is however necessary before confirming the utility of specific features for novel automatic spindle detectors.

The proposed features not only showed a likely utility in ruling out alpha waves, but also a similar ability (compared with RP in the sigma band) to discriminate between pre-spindle and spindle periods (such as TTV) or even showing higher classification statistics (e.g. SE in the sigma band), as shown in table 1. In fact, the conventional feature used in automatic spindle detectors (i.e. the RP in sigma band) only shows the highest statistics in specificity. Thus, SE is proposed as higher-performance candidate than RP for the detection of sleep spindles.

Except for PLE, the spectral features showed similar patterns of temporal evolution, with a flat trend in the pre-spindle and an increase for approximately 1 s after the spindle onset (see figure 3). On the contrary, both PLE and all temporal characteristics showed varied patterns in their trends that affected both the pre-spindle and spindle periods. This suggests that these features provide different information to that given by RP and SE. Therefore, although they have not reached a classification performance as high as RP or SE, it is well known that complementary features help in predictions leading to increased precision [64]. Not only that, but even the features that are presumably redundant with respect to RP could improve the prediction, since they would reduce the

noise getting consequently better inter-class separation [64].

Taken together, the results suggest that automatic spindle detectors could benefit from characterization through complementary measures both to discard alpha, and other oscillations and to increase algorithm sensitivity.

4.2. Limitations and future work

New ideas and suggestions for future spindle detectors were presented here. We demonstrate their potential utility by means of correlation between pre-spindle and spindle features, as well as by a classification procedure using ROCs. However, these ideas, although valid, are an indirect evidence, being the development of a new spindle detector based on the joint characterization of spectral and temporal measurements a more direct way to verify these findings. Therefore, future work is necessary in this regard to test the accuracy improvement due to each particular feature.

Apart from methodological suggestions for future detectors, clinical implications related to possible targets for boosting spindles were revealed. Nonetheless, these findings are limited at the cortical structures of the brain, since their activation was assessed by EEG signals. The typical spatial resolution of overnight EEG recordings, usually from PSGs, limit a source-level analysis. Simultaneous fMRI-EEG recordings could partially solve this problem, which would extend our findings about the strong state-dependence to the spindle generators as the thalamus. Although the recordings probably could not be overnight due to the discomfort of the fMRI equipment, this is a potentially promising priority to pursue it in future work.

Finally, we want to note that all the results of the present study are subject to the reliability and idiosyncrasies of the spindle detector employed here. In particular, the parameters associated with the detector, such as the threshold to consider the spindle onset, could slightly affect to the exact moment in which the spindle beginning is set. However, as previously mentioned, this automatic spindle detector has been widely validated by experts and non-experts, as well as compared to other approaches (e.g. [31, 35, 36, 65, 66]). Therefore, we are reasonably confident that the results are generalizable regardless of the spindle detection method.

5. Conclusion

The current definition of spindles is only based on power in the sigma band manifestation during the spindle period itself. However, the hierarchical complexity in which spindles are nested begins even before they are generated and makes necessary to characterize spindles in terms beyond power and

beyond the spindle period itself. By means of a correlation analysis and a classification procedure, the features computed in this study to characterize brain dynamics demonstrated their potential utility as predictors of spindles that could be applied to develop new automatic detectors and novel therapeutic targets aimed at improving memory, cognition and sleep quality in healthy, older, and clinical populations. In this regard, the SE calculated on the sigma band showed better accuracy and AROC than the power in this band, suggesting that, physiologically speaking, the temporal dynamics of the spindles are more complex than a simple stable oscillatory burst.

Acknowledgments

This work was supported by the ‘Ministerio de Ciencia, Innovación y Universidades—Agencia Estatal de Investigación’ and ‘European Regional Development Fund (FEDER)’ under Projects DPI2017-84280-R, PGC2018-098214-A-I00 and RTC-2017-6516-1, and by ‘CIBER in Bioengineering, Biomaterials and Nanomedicine (CIBER-BBN)’ through ‘Instituto de Salud Carlos III’ co-funded with FEDER funds.

ORCID iDs

Javier Gomez-Pilar  <https://orcid.org/0000-0001-7882-7890>

Gonzalo C Gutiérrez-Tobal  <https://orcid.org/0000-0002-1237-3424>

Jesús Poza  <https://orcid.org/0000-0001-8577-9559>

Roberto Hornero  <https://orcid.org/0000-0001-9915-2570>

References

- [1] Prerau M J, Brown R E, Bianchi M T, Ellenbogen J M and Purdon P L 2017 Sleep neurophysiological dynamics through the lens of multitaper spectral analysis *Physiology* **32** 60–92
- [2] Cantero J L and Atienza M 2005 The role of neural synchronization in the emergence of cognition across the wake-sleep cycle *Rev. Neurosci.* **16** 69–84
- [3] Acharya U R, Faust O, Kannathal N, Chua T and Laxminarayan S 2005 Non-linear analysis of EEG signals at various sleep stages *Comput. Methods Programs Biomed.* **80** 37–45
- [4] Kobayashi T, Misaki K, Nakagawa H, Madokoro S, Ihara H, Tsuda K, Umezawa Y, Murayama J and Isaki K 1999 Non-linear analysis of the sleep EEG *Psychiatry Clin. Neurosci.* **53** 159–61
- [5] Berry R B et al 2012 Rules for scoring respiratory events in sleep: update of the 2007 AASM manual for the scoring of sleep and associated events *J. Clin. Sleep Med.* **08** 597–619
- [6] Gorgoni M, Scarpelli S, Reda F and de Gennaro L 2020 Sleep EEG oscillations in neurodevelopmental disorders without intellectual disabilities *Sleep Med. Rev.* **49** 101224
- [7] Larson-Prior L J, Zempel J M, Nolan T S, Prior F W, Snyder A Z and Raichle M E 2009 Cortical network functional connectivity in the descent to sleep *Proc. Natl Acad. Sci.* **106** 4489–94
- [8] Fang Z, Sergeeva V, Ray L B, Viczko J, Owen A M and Fogel S M 2017 Sleep spindles and intellectual ability: epiphenomenon or directly related? *J. Cogn. Neurosci.* **29** 167–82
- [9] Fang Z, Ray L B, Owen A M and Fogel S M 2019 Brain activation time-locked to sleep spindles associated with human cognitive abilities *Front. Neurosci.* **13** 46
- [10] Antony J W, Schönauer M, Staresina B P and Cairney S A 2019 Sleep spindles and memory reprocessing *Trends Neurosci.* **42** 1–3
- [11] Fernandez L M J and Lüthi A 2020 Sleep spindles: mechanisms and functions *Physiol. Rev.* **100** 805–68
- [12] Staresina B P, Bergmann T O, Bonnefond M, van der Meij R, Jensen O, Deuker L, Elger C E, Axmacher N and Fell J 2015 Hierarchical nesting of slow oscillations, spindles and ripples in the human hippocampus during sleep *Nat. Neurosci.* **18** 1679–86
- [13] Axmacher N, Elger C E and Fell J 2008 Ripples in the medial temporal lobe are relevant for human memory consolidation *Brain* **131** 1806–17
- [14] Ngo H-V-V, Seibold M, Boche D C, Mölle M and Born J 2019 Insights on auditory closed-loop stimulation targeting sleep spindles in slow oscillation up-states *J. Neurosci. Methods* **316** 117–24
- [15] Cox R, Schapiro A C, Manoach D S and Stickgold R 2017 Individual differences in frequency and topography of slow and fast sleep spindles *Front. Hum. Neurosci.* **11** 433
- [16] D’Atri A, Novelli L, Ferrara M, Bruni O and de Gennaro L 2018 Different maturational changes of fast and slow sleep spindles in the first four years of life *Sleep Med.* **42** 73–82
- [17] Gottselig J M, Bassetti C L and Achermann P 2002 Power and coherence of sleep spindle frequency activity following hemispheric stroke *Brain* **125** 373–83
- [18] Laventure S, Pinsard B, Lungu O, Carrier J, Fogel S, Benali H, Lina J-M, Boutin A and Doyon J 2018 Beyond spindles: interactions between sleep spindles and boundary frequencies during cued reactivation of motor memory representations *Sleep* **41** zsy142
- [19] Gomez-Pilar J, Poza J, Bachiller A, Gómez C, Molina V and Hornero R 2015 Neural network reorganization analysis during an auditory oddball task in schizophrenia using wavelet entropy *Entropy* **17** 5241–56
- [20] Martínez-Cagigal V, Santamaría-Vázquez E and Hornero R 2019 Asynchronous control of P300-based brain–computer interfaces using sample entropy *Entropy* **21** 230
- [21] Bachiller A, Lubeiro A, Díez Á, Suazo V, Domínguez C, Blanco J A, Ayuso M, Hornero R, Poza J and Molina V 2015 Decreased entropy modulation of EEG response to novelty and relevance in schizophrenia during a P300 task *Eur. Arch. Psychiatry Clin. Neurosci.* **265** 525–35
- [22] Huang Z et al 2017 Is there a nonadditive interaction between spontaneous and evoked activity? Phase-dependence and its relation to the temporal structure of scale-free brain activity *Cereb. Cortex* **27** 1037–59
- [23] Golesorkhi M, Gomez-Pilar J, Tumati S, Maia F and Northoff G 2021 Temporal hierarchy of intrinsic neural timescales converges with spatial core-periphery organization *Commun. Biol.* **4** 277
- [24] Jiménez-García J, Gutiérrez-Tobal G C, García M, Kheirandish-Gozal L, Martín-Montero A, Álvarez D, del Campo F, Gozal D and Hornero R 2020 Assessment of airflow and oximetry signals to detect pediatric sleep apnea-hypopnea syndrome using AdaBoost *Entropy* **22** 670
- [25] Wolff A, di Giovanni D A, Gómez-Pilar J, Nakao T, Huang Z, Longtin A and Northoff G 2019 The temporal signature of self: temporal measures of resting-state EEG predict self-consciousness *Hum. Brain Mapp.* **40** 789–803
- [26] Zilio F et al 2020 Are intrinsic neural timescales related to sensory processing? Evidence from abnormal behavioral states *NeuroImage* **226** 117579

- [27] Warby S C, Wendt S L, Welinder P, Munk E G S, Carrillo O, Sorensen H B D, Jennum P, Peppard P E, Perona P and Mignot E 2014 Sleep-spindle detection: crowdsourcing and evaluating performance of experts, non-experts and automated methods *Nat. Methods* **11** 385–92
- [28] Tsanas A and Clifford G D 2015 Stage-independent, single lead EEG sleep spindle detection using the continuous wavelet transform and local weighted smoothing *Front. Hum. Neurosci.* **9** 181
- [29] Adamczyk M, Genzel L, Dresler M, Steiger A and Friess E 2015 Automatic sleep spindle detection and genetic influence estimation using continuous wavelet transform *Front. Hum. Neurosci.* **9** 624
- [30] LaRocco J, Franaszczuk P J, Kerick S and Robbins K 2018 Spindler: a framework for parametric analysis and detection of spindles in EEG with application to sleep spindles *J. Neural Eng.* **15** 066015
- [31] Ray L B, Sockeel S, Soon M, Bore A, Myhr A, Stojanoski B, Cusack R, Owen A M, Doyon J and Fogel S M 2015 Expert and crowd-sourced validation of an individualized sleep spindle detection method employing complex demodulation and individualized normalization *Front. Hum. Neurosci.* **9** 507
- [32] Nonclercq A, Urbain C, Verheulpen D, Decaestecker C, van Bogaert P and Peigneux P 2013 Sleep spindle detection through amplitude–frequency normal modelling *J. Neurosci. Methods* **214** 192–203
- [33] Wendt S L, Christensen J A E, Kempfner J, Leonthin H L, Jennum P and Sorensen H B D 2012 Validation of a novel automatic sleep spindle detector with high performance during sleep in middle aged subjects *2012 Annual Int. Conf. IEEE Engineering in Medicine and Biology Society (IEEE)* pp 4250–3
- [34] Delorme A and Makeig S 2004 EEGLAB: an open source toolbox for analysis of single-trial EEG dynamics including independent component analysis *J. Neurosci. Methods* **134** 9–21
- [35] Albouy G, Fogel S, King B R, Laventure S, Benali H, Karni A, Carrier J, Robertson E M and Doyon J 2015 Maintaining vs. enhancing motor sequence memories: respective roles of striatal and hippocampal systems *NeuroImage* **108** 423–34
- [36] Fogel S M *et al* 2014 fMRI and sleep correlates of the age-related impairment in motor memory consolidation *Hum. Brain Mapp.* **35** 3625–45
- [37] Bachiller A, Poza J, Gómez C, Molina V, Suazo V and Hornero R 2015 A comparative study of event-related coupling patterns during an auditory oddball task in schizophrenia *J. Neural Eng.* **12** 016007
- [38] Núñez P, Poza J, Bachiller A, Gomez-Pilar J, Lubeiro A, Molina V and Hornero R 2017 Exploring non-stationarity patterns in schizophrenia: neural reorganization abnormalities in the alpha band *J. Neural Eng.* **14** 046001
- [39] Gomez-Pilar J, Northoff G, Vaquerizo-Villar F, Poza J, Gutiérrez-Tobal G C and Hornero R 2020 Intraindividual characterization of the sleep spindle variability in healthy subjects *42nd Annual Int. Conf. IEEE Engineering in Medicine and Biology Society (Montreal, Canada)* 3473–76
- [40] Welch P 1967 The use of fast Fourier transform for the estimation of power spectra: a method based on time averaging over short, modified periodograms *IEEE Trans. Audio Electroacoust.* **15** 70–73
- [41] Wamsley E J, Tucker M A, Shinn A K, Ono K E, McKinley S K, Ely A V, Goff D C, Stickgold R and Manoach D S 2012 Reduced sleep spindles and spindle coherence in schizophrenia: mechanisms of impaired memory consolidation? *Biol. Psychiatry* **71** 154–61
- [42] Schabus M *et al* 2007 Hemodynamic cerebral correlates of sleep spindles during human non-rapid eye movement sleep *Proc. Natl Acad. Sci.* **104** 13164–9
- [43] Inouye T, Shinosaki K, Sakamoto H, Toi S, Ukai S, Iyama A, Katsuda Y and Hirano M 1991 Quantification of EEG irregularity by use of the entropy of the power spectrum *Electroencephalogr. Clin. Neurophysiol.* **79** 204–10
- [44] Gomez-Pilar J, García-Azorín D, Gomez-lopez-de-san-roman C, Guerrero Á L and Hornero R 2020 Exploring EEG spectral patterns in episodic and chronic migraine during the interictal state: determining frequencies of interest in the resting state *Pain Med.* **21** 3530–38
- [45] Fernández A, Ríos-Lago M, Abásolo D, Hornero R, Álvarez-Linera J, Paul N, Maestú F and Ortiz T 2011 The correlation between white-matter microstructure and the complexity of spontaneous brain activity: a diffusion tensor imaging-MEG study *NeuroImage* **57** 1300–7
- [46] Maturana-Candelas A, Gómez C, Poza J, Pinto N and Hornero R 2019 EEG characterization of the Alzheimer's disease continuum by means of multiscale entropies *Entropy* **21** 544
- [47] Hornero R, Aboy M and Abásolo D 2007 Analysis of intracranial pressure during acute intracranial hypertension using Lempel–Ziv complexity: further evidence *Med. Biol. Eng. Comput.* **45** 617–20
- [48] Aboy M, Hornero R, Abasolo D and Alvarez D 2006 Interpretation of the Lempel–Ziv complexity measure in the context of biomedical signal analysis *IEEE Trans. Biomed. Eng.* **53** 2282–8
- [49] Nagarajan R 2002 Quantifying physiological data with Lempel–Ziv complexity—certain issues *IEEE Trans. Biomed. Eng.* **49** 1371–3
- [50] Lake D E, Richman J S, Griffin M P and Moorman J R 2002 Sample entropy analysis of neonatal heart rate variability *Am. J. Physiol. Integr. Comp. Physiol.* **283** R789–97
- [51] Richman J S and Moorman J R 2000 Physiological time-series analysis using approximate entropy and sample entropy *Am. J. Physiol. Heart. Circ. Physiol.* **278** H2039–49
- [52] Cohen M E, Hudson D L and Deedwania P C 1996 Applying continuous chaotic modeling to cardiac signal analysis *IEEE Eng. Med. Biol. Mag.* **15** 97–102
- [53] Zerouali Y, Lina J-M, Sekerovic Z, Godbout J, Dube J, Jolicoeur P and Carrier J 2014 A time-frequency analysis of the dynamics of cortical networks of sleep spindles from MEG-EEG recordings *Front. Neurosci.* **8** 310
- [54] Schönwald S V, Carvalho D Z, Dellagustin G, de Santa-helena E L and Gerhardt G J L 2011 Quantifying chirp in sleep spindles *J. Neurosci. Methods* **197** 158–64
- [55] Honey C J, Theisen T, Donner T H, Silbert L J, Carlson C E, Devinsky O, Doyle W K, Rubin N, Heeger D J and Hasson U 2012 Slow cortical dynamics and the accumulation of information over long timescales *Neuron* **76** 423–34
- [56] Zweig M H and Campbell G 1993 Receiver-operating characteristic (ROC) plots: a fundamental evaluation tool in clinical medicine *Clin. Chem.* **39** 561–77
- [57] Efron B and Tibshirani R J 1994 *An Introduction to the Bootstrap* (New York: Chapman and Hall/CRC)
- [58] Witten I H, Frank E, Hall M A and Pal C J 2016 *Data Mining: Practical Machine Learning Tools and Techniques* (Cambridge: Elsevier) (<https://doi.org/10.1016/C2015-0-02071-8>)
- [59] Benjamini Y and Hochberg Y 1995 Controlling the false discovery rate: a practical and powerful approach to multiple testing *J. R. Stat. Soc.* **57** 289–300
- [60] Helfrich R F, Mander B A, Jagust W J, Knight R T and Walker M P 2018 Old brains come uncoupled in sleep: slow wave–spindle synchrony, brain atrophy, and forgetting *Neuron* **97** 221–30.e4
- [61] Palva S and Palva J M 2007 New vistas for α -frequency band oscillations *Trends Neurosci.* **30** 150–8
- [62] Pivik R T and Harman K 1995 A reconceptualization of EEG alpha activity as an index of arousal during sleep: all alpha activity is not equal *J. Sleep Res.* **4** 131–7
- [63] Carvalho D Z, Gerhardt G J L, Dellagustin G, de Santa-helena E L, Lemke N, Segal A Z and Schönwald S V 2014 Loss of sleep spindle frequency deceleration in obstructive sleep apnea *Clin. Neurophysiol.* **125** 306–12
- [64] Igyuon I and Elisseeff A 2003 An introduction to variable and feature selection *J. Mach. Learn. Res.* **3** 1157–82

- [65] Laventure S, Fogel S, Lungu O, Albouy G, Sévigny-Dupont P, Vien C, Sayour C, Carrier J, Benali H and Doyon J 2016 NREM2 and sleep spindles are instrumental to the consolidation of motor sequence memories *PLoS Biol.* **14** e1002429
- [66] Fogel S, Vien C, Karni A, Benali H, Carrier J and Doyon J 2017 Sleep spindles: a physiological marker of age-related changes in gray matter in brain regions supporting motor skill memory consolidation *Neurobiol. Aging* **49** 154–64